

# Novel synthesis and characterization of nanocomposite Pt-WO<sub>3</sub>-TiO<sub>2</sub>/C electrocatalyst for PEMFC

M. Nagarajan · G. Paruthimal Kalaiganan ·  
G. A. Pathanjali

Received: 27 November 2010 / Revised: 10 March 2012 / Accepted: 1 April 2012 / Published online: 27 April 2012  
© Springer-Verlag 2012

**Abstract** In this study, an effective preparation of Pt-WO<sub>3</sub>-TiO<sub>2</sub>/C electrocatalysts has been developed for polymer electrolyte membrane fuel cell (PEMFC) application. The single cell performance of Vulcan XC-72R carbon-supported Pt-WO<sub>3</sub>-TiO<sub>2</sub> electrocatalysts with various compositions (as weight percentage Pt-W-Ti 0:5:5, 2:4:4, 4:3:3, 6:2:2, and 8:1:1) as anode materials are investigated in PEMFC. These catalysts are compared with 10 % Pt/C on the same Vulcan XC-72R carbon support and 10 % Pt/C (commercial) electrocatalyst. The physical and morphological characterization of the optimized Pt-WO<sub>3</sub>-TiO<sub>2</sub>/C, 10 % Pt/C, and 10 % Pt/C (commercial) electrocatalysts are further investigated by X-ray diffraction (XRD), cyclic voltammetry, scanning electron microscopy with energy-dispersive X-ray analysis, and transmission electron microscopy (TEM) techniques. Among all the molar ratio of the catalysts, the Pt-W-Ti (4:3:3) molar ratio catalyst exhibited the larger electrochemical active surface area. The electrochemical performance of Pt-WO<sub>3</sub>-TiO<sub>2</sub>/C (with a weight percentage of Pt-W-Ti 4:3:3) as anode material is better than those of other compositions of Pt-WO<sub>3</sub>-TiO<sub>2</sub>/C catalysts. The amount of platinum was also reduced from 1.76 to 0.704 mg cm<sup>-2</sup> which exhibited higher performance in single cell tests. Platinum shows a smaller-sized crystalline structure in XRD and TEM analysis. High performance indicates that enhanced proton transport occurs through the use of this catalyst.

**Keyword** Nanostructures · Chemical synthesis · X-ray diffraction · Transition electron microscopy

## Introduction

Fuel cells are attractive power sources for both stationary and electric vehicle applications due to their high conversion efficiencies and low pollution. Among the various types of fuel cells, the proton exchange membrane fuel cells (PEMFC) are the most suitable candidates for electric vehicles as they can be operated at a low temperature of less than 100 °C. Platinum supported on carbon black is widely used as the electrocatalyst in PEMFC. However, platinum is expensive, and the world's supply of Pt is limited. Therefore, improving the electrocatalytic activity of platinum with minimum loading level is important. The search for hydrogen oxidation reaction (HOR) catalysts that are more active, less expensive, and with greater stability than platinum has resulted in the development of Pt alloys. From both the scientific and the technological point of view, binary and ternary nanoparticles composed of two or three different metal elements are of greater interest and importance than monometallic nanoparticles. Scientists have especially focused on binary and ternary nanoparticles as catalysts in view of their novel catalytic behaviors exhibited by the addition of the second or third metal element. This effect of the second and third metal element can often be explained in terms of an ensemble and a ligand effect in catalysis. Some platinum-based binary and ternary alloys such as Pt-Ni, Pt-Ru-Ni, Pt-Mo, and Pt-Cr exhibit a higher catalytic activity for HOR than pure platinum [1–3]. Chen et al. synthesized Pt-Ru/WO<sub>3</sub>/C by freeze drying method and investigated the low poisoning rate of CO on Pt-Ru/WO<sub>3</sub>/C [4]. Anode and cathode electrocatalysts in PEM fuel cells are predominantly carbon-supported, platinum-

G. A. Pathanjali (✉)  
High Energy Batteries (I) Ltd.,  
Mathur 622515, India  
e-mail: pudumunag@gmail.com

M. Nagarajan · G. Paruthimal Kalaiganan  
Department of Industrial Chemistry, Alagappa University,  
Karaikudi 630003, India

**Table 1** Composition of elements in the different catalysts

Element	Type “A”	Type “B”	Type “C”	Type “D”	Type “E”	Type “F”
Pt %	0	2	4	6	8	10
WO <sub>3</sub> as W%	5	4	3	2	1	0
TiO <sub>2</sub> as Ti%	5	4	3	2	1	0

based alloy nanoparticles, with particle sizes typically in the range of 1–3 nm. The high dispersion provides the advantage of high specific surface areas and utilization of the precious metals [5]. The unique advantage is the lowering of the precious metal loading achieved by increasing the surface area of the active site of the electrocatalyst [6]. Li et al. [7] reported that the Pt/tourmaline nanocomposite is catalytically more active and stable than platinum-modified glassy carbon electrode for electrooxidation of methanol and also the current density was significantly enhanced. Rajalakshmi et al. [8] have reported that the presence of TiO<sub>2</sub> in the Pt matrix is likely to prevent the agglomeration of Pt particles and effectively dispersed the Pt atoms in the cluster. It also controls the nanostructure of the catalyst and provides thermal and oxidation stability with respect to corrosion.

In this present work, carbon-supported Pt-WO<sub>3</sub>-TiO<sub>2</sub> nanocomposite with various compositions of Pt-WO<sub>3</sub>-TiO<sub>2</sub> (as weight percentage, Pt-W-Ti 0:5:5, 2:4:4, 4:3:3, 6:2:2, 8:1:1, and 10:0:0) were prepared by sodium borohydride reduction method for use as anode electrocatalysts. The novel approach followed for doping of WO<sub>3</sub> and TiO<sub>2</sub> into Pt particles has been fully established. The technique followed in this work for the inclusion of oxides of second and third elements into platinum prevents the agglomeration of platinum particles. Evaluation was carried out to compare the single cell performance in PEMFC, and the optimized Pt-WO<sub>3</sub>-TiO<sub>2</sub> composition was further characterized for its particle size, specific surface area, and electrochemical surface area. Comparison of data obtained with that of 10 % Pt/C and commercial 10 % Pt/C (Arora) electrocatalysts was attempted using X-ray diffraction (XRD), cyclic voltammetry (CV), SEM, energy-dispersive X-ray (EDX), and transmission electron microscopy (TEM) techniques. The effects of inclusion of WO<sub>3</sub>-TiO<sub>2</sub> molecules on platinum are discussed.

## Experimental

### Preparation of Pt-WO<sub>3</sub>-TiO<sub>2</sub>/C and 10 % Pt/C electrocatalyst

Six types of electrocatalysts (refer to Table 1) were prepared by chemical method. All six types of catalysts were prepared as follows: electrocatalysts type “B” to “E” were prepared using calculated volume of hydrogen

hexachloroplatinate (IV), and Ti<sub>2</sub>(SO<sub>4</sub>)<sub>3</sub> aqueous solutions were added to Vulcan XC-72R carbon black and were mixed well. The metal-containing carbon slurry mixer was subjected to ultrasonic vibration for 45 min at room temperature, and pH of the slurry was adjusted to 9 by adding 1 N NaOH solution and heated to 65±5 °C. Subsequently, excess quantity of 1 % sodium borohydride solution (reducing agent) was added dropwise to the carbon slurry catalyst mixer with constant stirring. Temperature was maintained at 65±5 °C and allowed to stand for 1 h to complete the reaction. The resultant catalyst slurry was centrifuged and washed with double distilled water till the final wash water pH reached 7.5. Calculated volume of sodium tungstate (Merck) aqueous solution was added to the washed slurry, and the pH was reduced to 0.5 by adding HCl (Merck) and heated to 65±5 °C for 1 h with constant stirring. For type “A,” addition of hydrogen hexachloroplatinate (IV) was not done to prepare a control without Pt content; similarly, type “F” was prepared as a control with Pt content only, and hence, Ti and W metal precursor solutions were not added. The above six types of catalyst slurries were centrifuged and washed with double distilled water. Finally, well-washed catalyst slurry was dried at 110±5 °C for 4 h. The wash water was analyzed for Pt, W, and Ti metal ions. There was no trace of metal ion present, indicating complete reduction of metal.

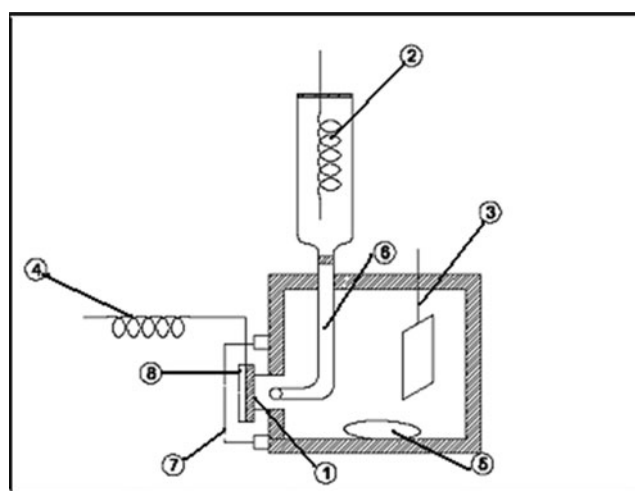
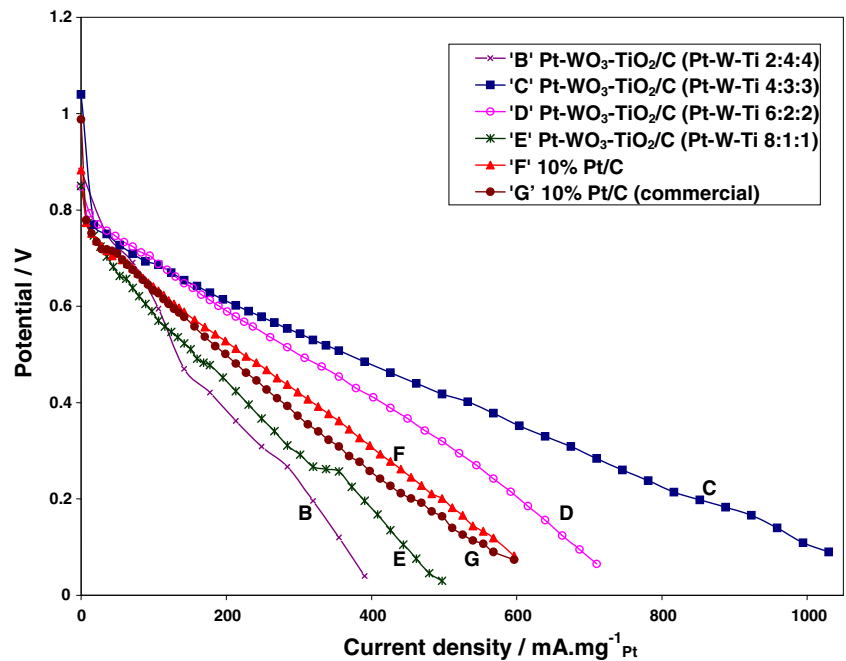


**Fig. 1** Typical electrochemical cell setup: 1 working electrode, 2 silver–silver chloride electrode, 3 counter electrode, 4 electrical contact, 5 Teflon-coated magnetic bar, 6 luggin, 7 working electrode holder, 8 circular silver foil

**Fig. 2** Comparison of the I-V polarization performance of the single cell PEMFC with various catalysts



Electrochemical characterization

Single cell performance test

One hundred ten milligrams of carbon-supported catalyst, 0.53 ml of 5 % Nafion® (Dupont), and 0.94 ml of isopropyl alcohol were mixed and subjected to ultrasonic vibration for 1 h. The prepared homogeneous slurry was transferred completely to one side of the PTFE-coated (wet proof) carbon sheet E-TEK® and rolled using stainless steel roller to get smooth finish of the catalyst layer on the carbon sheet. After the rolling operation, it was observed that the catalyst loss was about 10 %. To compensate for the loss, additional catalyst (10 %) was

introduced in the catalyst mixer. Two hundred microliters of 5 % Nafion® (Dupont) was uniformly dispersed on the surface of the catalyst layer and dried for 8 h at room temperature in vacuum desiccators. Finally, the electrodes were dried at  $110 \pm 5$  °C for 4 h. In total, six types of prepared catalysts and one commercial 10 % Pt/C catalyst were used for making the anodes. M/s High Energy Batteries (India) Ltd. supplied the cathode, which formed part of membrane electrode assembly (MEA) in all cells. Commercial polymer electrolyte membranes (Nafion 117®; Dupont) were treated sequentially at 80 °C for 1 h in each of the following solutions [4]: 5 % H<sub>2</sub>O<sub>2</sub> solution, deionized water (DI), and 0.5 M H<sub>2</sub>SO<sub>4</sub> acid solution. Finally, they were washed thoroughly with DI water

**Fig. 3** Power density against current density curves recorded in the PEMFC single cell with various catalysts

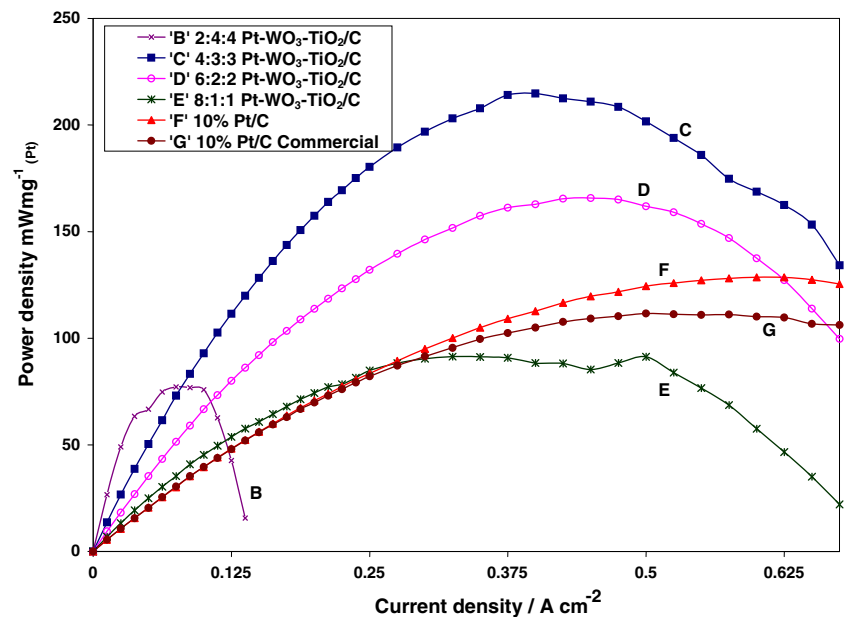


**Table 2** Single cell performance results of the various anode electrodes

Type	Anode electrode catalyst material	Pt content in the anode $\text{mg cm}^{-2}$	Maximum power density $\text{mW mg}^{-1}$ (Pt)
B	Pt-WO <sub>3</sub> TiO <sub>2</sub> /C (Pt-W-Ti; 2:4:4)	0.352	202
C	Pt -WO <sub>3</sub> -TiO <sub>2</sub> /C (Pt-W-Ti; 4:3:3)	0.704	215
D	Pt-WO <sub>3</sub> -TiO <sub>2</sub> /C (Pt-W-Ti; 6:2:2)	1.056	165
E	Pt-WO <sub>3</sub> -TiO <sub>2</sub> /C (Pt-W-Ti; 8:1:1)	1.408	91
F	10 % Pt/C	1.760	128
G	10 % Pt/C (commercial)	1.760	111

Power density value is based on the platinum content

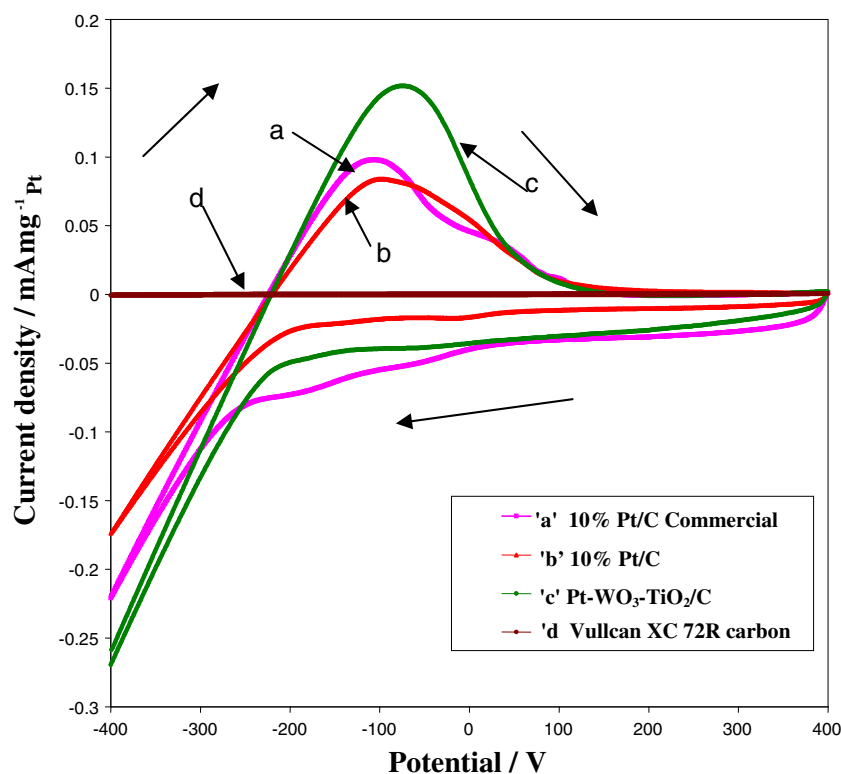
to neutral pH and air dried. The seven types of MEA samples were formed. The treated Nafion 117® (Dupont) membrane was placed between the anode and cathode and thereafter hot pressed at 130 °C under the pressure of 50 kg cm<sup>-2</sup> for 3 min [9–11]. MEA was then placed between graphite manifold plates, machined with a serpentine flow channel. Humidified hydrogen was fed at a flow rate of 60 ml min<sup>-1</sup> at 70 °C to anode side, and oxygen was fed at a flow rate of 80 ml min<sup>-1</sup> at 65 °C to cathode side. The geometric area of the electrode was 4 cm<sup>2</sup>, and no external heating was provided to the cell. The applied load current was increased periodically every 3 min, and the corresponding potentials were recorded under steady state. Single cell test station was constructed in-house, with the needed provisions for humidified gas supplies (hydrogen and

oxygen) with the following calibrated instruments: gas flow meter, Power source (APLAB, India), and E2373A Hewlett Packard Digital multimeters.

#### Cyclic voltammetry

The catalyst ink was prepared by dispersing 10 mg of catalyst in 1 ml of isopropyl alcohol containing 50  $\mu\text{l}$  of Nafion® emulsion, and this was subjected to ultrasonic vibration for 45 min. Thus, prepared ink of 200  $\mu\text{l}$  was uniformly dispersed on smooth graphite sheet and allowed to dry in a vacuum dessicator for 2 h. Thus, 75  $\mu\text{l}$  of 0.5 % Nafion® emulsion was uniformly dispersed on the coated catalyst layer, and this was allowed to dry in air, followed by final drying at 110 °C for

**Fig. 4** Cyclic voltammetry curves for the various catalysts in 0.5 M H<sub>2</sub>SO<sub>4</sub> at room temperature. Ag/AgCl electrode was used as a reference electrode, and platinum was used as a counter electrode. The potential scan was at 50 mV s<sup>-1</sup> *a* 10 % Pt/C commercial catalyst, *b* 10 % Pt/C, *c* Pt-WO<sub>3</sub>-TiO<sub>2</sub>/C (Pt/W/Ti, 4:3:3) and *d* Vulcan XC-72R carbon



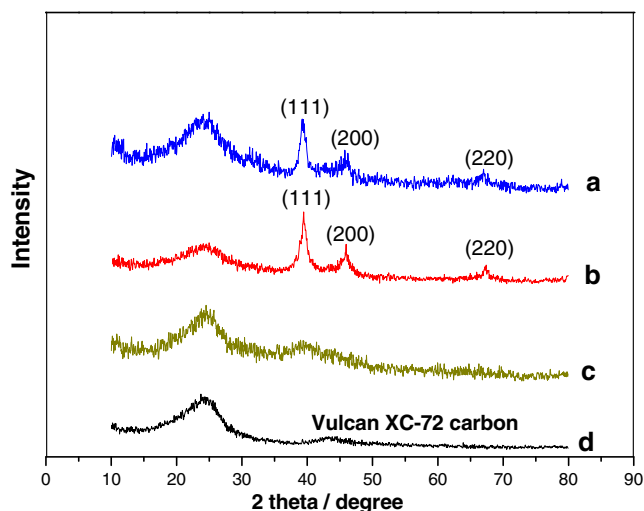


**Fig. 5** X-ray diffraction patterns of catalysts *a* Pt-WO<sub>3</sub>-TiO<sub>2</sub> (Pt/W/Ti, 4:3:3), *b* 10 % Pt/C, *c* 10 % Pt/C commercial catalyst, and *d* Vulcan XC-72R carbon

1 h, and then, the electrodes were kept in a vacuum desiccator for 1 h. Electrochemical measurements were carried out by cyclic voltammetry using a potentiostat (BAS 100B). Three-electrode cell assembly (Fig. 1) consisting of a thin smooth graphite sheet coated with catalyst layer of 1 cm<sup>2</sup> was used as working electrode. Platinum black-coated platinum was used as counter electrode and silver–silver chloride electrode used as reference electrode. Graphite sheet served as an underlying substrate for the working electrode. The voltammetry experiments were performed in 0.5 M H<sub>2</sub>SO<sub>4</sub> electrolyte solution at room temperature. Argon gas was purged into the electrolyte for about 15 min to remove dissolved oxygen before starting the experiment. Stable voltammograms were recorded after scanning for 10 cycles in the potential range from –400 to +400 mV at a scan rate of 50 mV s<sup>–1</sup>.

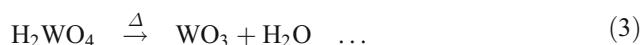
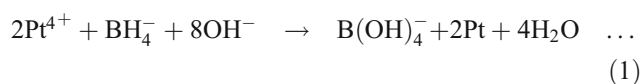
#### Physical characterization measurements

XRD investigation was carried out with X’Pert PRO diffractometer using crystal monochromatized CuKα-1 radiation of 40 kV and 30 mA. Step scans were conducted between 10° and 80° (2θ) using a 0.05° step size and a scan step time of 10.1. The surface morphology of the surfaces of the Pt-WO<sub>3</sub>-TiO<sub>2</sub>/C, 10 % Pt/C, and 10 % Pt/C commercial catalysts was investigated with a JEOL JSM-6360 SEM at

an accelerating potential of 25 kV. The chemical composition at the surface of catalysts was determined by EDX coupled with the scanning electron microscope. The catalyst samples were finely ground and ultrasonically dispersed in isopropyl alcohol, and a drop of the prepared dispersion was deposited and dried on standard copper grid, and nano-sized particles of the optimized Pt-WO<sub>3</sub>-TiO<sub>2</sub>/C, 10 % Pt/C, and 10%Pt/C commercial catalysts were investigated with a Philips CM200 transmission electron microscope with an operating voltage of 100 kV and a resolution of 2.4 Å.

## Results and discussion

During the following chemical reaction, Pt-WO<sub>3</sub>-TiO<sub>2</sub> composite and Pt particles get dispersed on the carbon support, while initially platinum ions reduce as Pt on the surface of carbon particle, Eq. (1) [12]. Sodium tungstate gets precipitated as hydrated tungstic oxide (WO<sub>3</sub>xH<sub>2</sub>O) within the platinum particles, Eq. (2), and loses water molecules after heating.



Titanium IV sulfate gives a white gelatinous precipitate of metatitanic acid, H<sub>2</sub>TiO<sub>3</sub>, and further converts into titanium IV oxide (stable) [13]. The formation of titanium (IV) hydroxide precedes the earlier reaction, and titanium IV oxide is formed on drying within the platinum particles.

#### Electrochemical characterization

##### Single cell performance

The cell polarization and power density curves of the PEMFC with various anode catalysts are shown in Figs. 2 and 3. The Pt-WO<sub>3</sub>-TiO<sub>2</sub>/C (type “C”) anode catalyst exhibits the highest cell

**Table 3** Crystallographic data of various prepared anode catalysts obtained from XRD pattern

Catalyst	2θ (°) (220)	Lattice parameter (nm)	FWHM (2θ)	Particle size (nm)	specific area (m <sup>2</sup> g <sup>–1</sup> )
Pt-WO <sub>3</sub> -TiO <sub>2</sub> /C (Pt-W-Ti 4:3:3) type “C”	68.29	0.3881	3.9000	2.46	113.9
Pt/C type “F”	67.15	0.3939	3.5326	2.7	103.8
Pt/C (commercial) type “G”	No peak	–	–	–	–



potential and power density under same discharging current (Fig. 2). Catalyst type “A” ( $\text{WO}_3\text{-TiO}_2/\text{C}$ ) did not show the I-V performance due to the absence of Pt. The maximum power density obtained was  $215 \text{ mW mg}_{(\text{Pt})}^{-1}$  compared to other anodes prepared using commercial catalysts. Pt- $\text{WO}_3\text{-TiO}_2/\text{C}$  (type “C”) catalyst shows higher power density (Table 2) than commercial 10 % Pt/C catalyst and prepared 10 % Pt/C catalyst (Fig. 3). Pt- $\text{WO}_3\text{-TiO}_2/\text{C}$  (type “C”) catalyst also showed better performance than the other Pt- $\text{WO}_3\text{-TiO}_2/\text{C}$  (“A,” “B,” “D,” and “E”), commercial 10 % Pt/C, and prepared 10 % Pt/C (type “F”). It is evident that, inclusion of the particular ratio of tungstate molecules into the platinum particles improves the adsorption of hydrogen and dissociation of hydrogen molecule into protons. Somewhat exotic approach based on Nafion is the incorporation of  $\text{WO}_3$  and  $\text{TiO}_2$  into the Pt particles. Pt is believed to catalyze the recombination of hydrogen and oxygen inside the membrane, providing an “internal humidification,” while the metal oxides are thought to retain water within the membrane [14] and enhances the proton conductivity at the anode side. The technique followed in this work for the inclusion of second and third elements into platinum prevents the agglomeration of platinum particle. The electrochemical experiments were carried out repeatedly, and the results were consistent. Actually, the ratio of Pt- $\text{WO}_3\text{-TiO}_2$  (4:3:3) is an optimized composition. The hydrogen adsorption and desorption steps were processed on the available surface area. On Pt- $\text{WO}_3\text{-TiO}_2$  (2:4:4), the surface area becomes less due to the high composition of W and Ti metal oxides. This, in turn, restricts the proton conductivity. In the case of Pt- $\text{WO}_3\text{-TiO}_2$  (8:1:1), the activity of  $\text{WO}_3$  and  $\text{TiO}_2$  was less due to the presence of insufficient amount of these composite materials. While the proton conductivity is more due to higher Pt levels, humidification of electrocatalytic site limits the performance. The optimized Pt- $\text{WO}_3\text{-TiO}_2/\text{C}$  (Pt-W-Ti 4:3:3), 10 % Pt/C, and 10 % Pt/C (commercial) catalysts were further characterized using CV, XRD, SEM with EDX, and TEM techniques.

#### Cyclic voltammetry

Figure 4 shows that the cyclic voltammetry curves for Pt- $\text{WO}_3\text{-TiO}_2/\text{C}$  (type “C”), 10 % Pt/C, and 10 % Pt/C (commercial) catalysts in 0.5 M  $\text{H}_2\text{SO}_4$  solution. The potential for hydrogen adsorption/desorption curves, peak current densities, and the peak potentials were about  $0.152 \text{ mA mg}^{-1}$ ;  $-71 \text{ mV}$ , for Pt- $\text{WO}_3\text{-TiO}_2/\text{C}$  (type “C”),  $0.084 \text{ mA mg}^{-1}$ ;  $-95 \text{ mV}$  for Pt/C (“F”), and  $0.098 \text{ mA mg}^{-1}$ ;  $-105 \text{ mV}$  for Pt/C (commercial) catalysts. Higher peak currents were observed for Pt- $\text{WO}_3\text{-TiO}_2/\text{C}$  (type “C”) catalysts when compared to lone Pt catalysts. The charges under the voltammetric peaks for hydrogen adsorption or desorption correspond to adsorption of one hydrogen atom on each metal surface ( $Q_{\text{H}}$ ). The charges associated with one-to-one H-M correspondence per unit surface area are calculated on the basis of the distribution of metal

atoms over the surface. The electrochemical surface areas (ESA) for the Pt- $\text{WO}_3\text{-TiO}_2/\text{C}$ , Pt/C, and Pt/C (commercial) catalysts were determined by integrating the charge of the

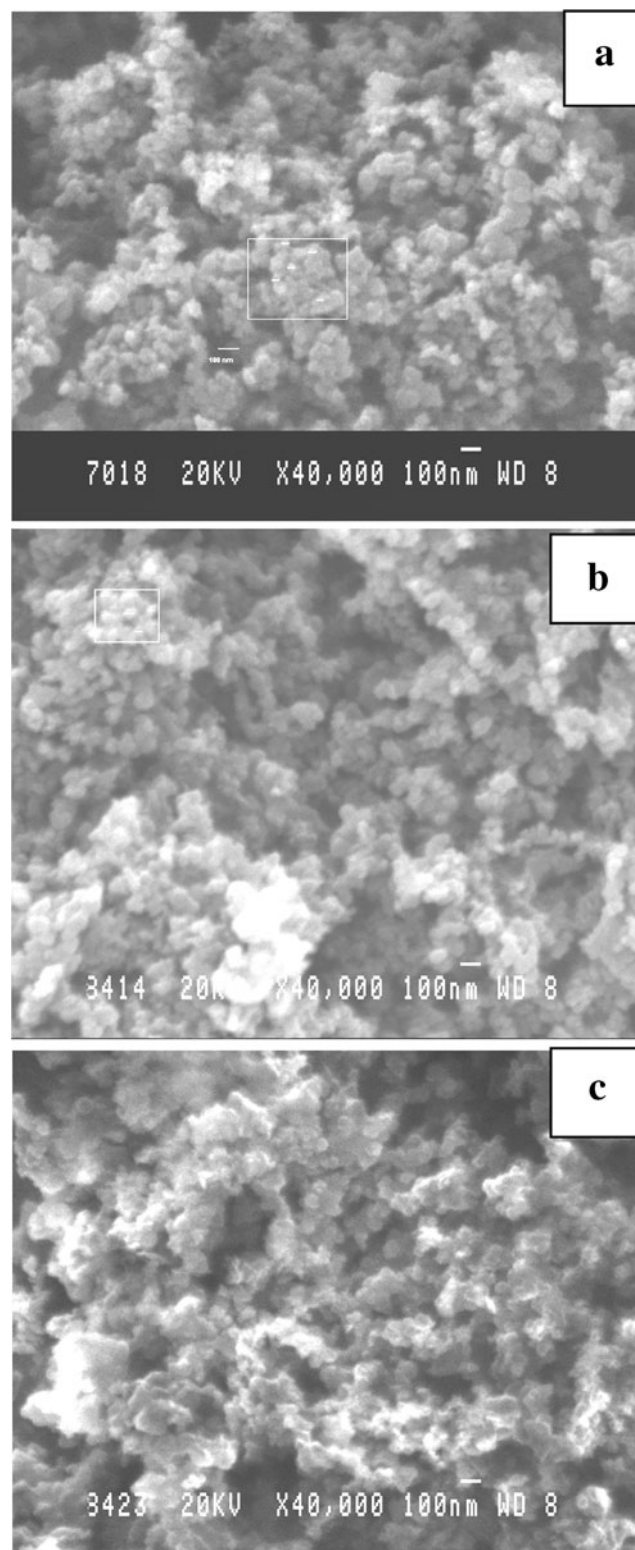


**Fig. 6** SEM images of catalysts: **a** Pt- $\text{WO}_3\text{-TiO}_2/\text{C}$  (Pt/W/Ti, 4:3:3), **b** 10 % Pt/C, and **c** 10 % Pt/C commercial catalysts

**Table 4** Energy-dispersive X-ray spectroscopic data of optimized catalyst Pt-WO<sub>3</sub>-TiO<sub>2</sub>/C type “C” element composition

Element	Weight <sup>a</sup> %	Atomic <sup>a</sup> %
W (M)	28.95	61.8
Ti (M)	30.03	16.7
Pt (M)	41.02	21.5

<sup>a</sup><2 sigma

hydrogen desorption region ( $Q_H$ ), Eq. (4), assuming that the polycrystalline Pt electrode gave hydrogen desorption charge of  $0.21 \times 10^{-3} \text{ C cm}^{-2}$  [15, 16].

ESA (square meters per gram)

$$= Q_H / (2.1C \times \text{g of platinum catalyst}) \dots \quad (4)$$

The calculated ESA values for Pt-WO<sub>3</sub>-TiO<sub>2</sub>/C (Pt-W-Ti 4:3:3), 10 % Pt/C, and 10 % Pt/C (commercial) catalysts

were 105, 79, and 74  $\text{m}^2 \text{ g}^{-1}$ , respectively, and these results were correlated with BET surface area [6] of carbon-supported catalyst. From the results, it is clear that the ESA values are higher for Pt-WO<sub>3</sub>-TiO<sub>2</sub>/C (type “C”) than lone Pt catalyst because of the presence of relatively smaller size of Pt. Besides, hydrogen atoms’ adsorption site also increased on the surface of the Pt particles.

Physical characterization of prepared and commercial catalysts

Figure 5 shows the XRD patterns of prepared and commercial electrocatalysts. All the XRD patterns displayed the (111), (200), (220) reflection characteristic of platinum face-centered cubic (fcc) crystal structure, except the commercial electrocatalyst. There was no relevant peak observed in the commercial catalyst. It is inferred that this catalyst is in amorphous state. The particle size ( $d$ ) of the catalysts was evaluated from the X-ray diffraction peaks (at

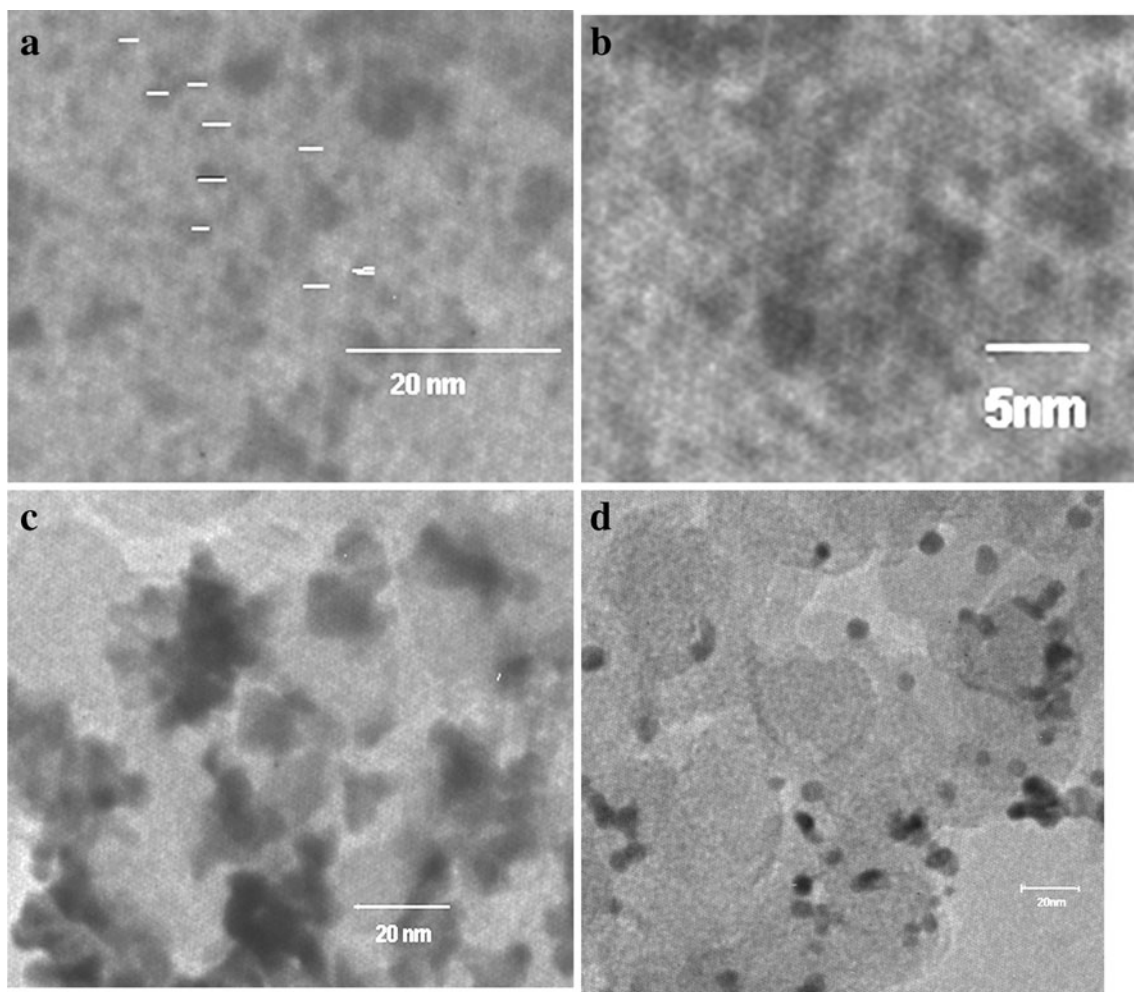


**Fig. 7** TEM images of prepared and commercial catalysts: **a** LMTEM of Pt-WO<sub>3</sub>-TiO<sub>2</sub>/C (4:3:3), **b** HMTEM of Pt-WO<sub>3</sub>-TiO<sub>2</sub>/C (4:3:3), **c** 10 % Pt/C, and **d** 10 % Pt/C commercial catalysts

220 plane) using the following Debye–Scherrer formula (5) [17–19].

$$d = k\lambda / (\beta_{1/2} \times \cos\theta_{\max}) \quad (\text{nanometers}) \quad \dots \quad (5)$$

where,  $d$  is the average particle size (nanometers),  $\lambda$  the wave length of X-ray (0.15406 nm),  $\theta$  is the angle (220) at which the peak maximum occurs,  $\beta_{1/2}$  the width (in radian) of the diffraction peak at a half height,  $k$  is the coefficient 0.89–1.39 (here 0.9). The equation for the relation between the catalyst spherical size and its surface area ( $S$ ) [20] may be expressed by

$$S = 6,000/\rho d \quad (\text{m}^2\text{g}^{-1}) \quad \dots \quad (6)$$

$\rho$  is the density of Pt metal, and  $d$  value was arrived from the formula in Eq. (5). Lattice parameter “ $a_{\text{fcc}}$ ” of platinum was calculated from Eq. (7) [9].

$$a_{\text{fcc}} = \sqrt{2\lambda_{\text{k}\alpha 1} / \sin\theta_{\max}} \quad (\text{nanometers}) \quad \dots \quad (7)$$

where,  $a_{\text{fcc}}$  = the lattice parameter,  $\lambda_{\text{k}\alpha 1}$  is the wavelength of crystal monochromatic Cu radiation, (0.15406 nm), and  $\theta_{\max}$  is the Bragg angle (220) plane. The values of particle size, surface area, and lattice parameter are tabulated in Table 3. The lattice parameters obtained for Pt-WO<sub>3</sub>-TiO<sub>2</sub>/C catalyst are smaller than those for 10 % Pt/C. In fact, the decrease in lattice parameters of the composite catalysts reflects the progressive increase in the incorporation of tungstate and titanate molecules into the composite state. The lattice parameter of prepared catalysts is about 0.39 nm, which is close to the XRD pattern of pure platinum. Pt-WO<sub>3</sub>-TiO<sub>2</sub> (“C”) and Pt/C (“F”) catalysts showed nano-sized platinum particles produced on carbon substrate material. The structure of W and Ti did not appear in the XRD pattern of catalysts, suggesting the absence of metallic W and Ti. The peaks associated with pure metallic W and Ti are not present in the pattern, indicating the presence of its oxides in amorphous state. The single cell performance is good in Pt-WO<sub>3</sub>-TiO<sub>2</sub> (type “C”) catalyst. Based on the results, it is proved that the crystalline structure of the catalyst is the predominant factor in determining the higher electrocatalytic activity. Typical scanning electron microstructures (SEM) of the catalyst particle are shown in Fig. 6, wherein the image of catalysts shows that catalyst particles were well dispersed on 30–40-nm size carbon-supported material. Typical EDX values of the chemical compositions of Pt, W, and Ti were given in Table 4. The EDX analysis showed that the determined composition is quite similar to the theoretical value. Chloroplatinate, sodium tungstate, and titanium IV sulfate as precursors were completely converted to Pt, WO<sub>3</sub>, and TiO<sub>2</sub> as composite material, respectively. The TEM images of Pt-WO<sub>3</sub>-TiO<sub>2</sub>/C electrocatalyst are shown in Fig. 7. It is inferred that dark particle represents the platinum particles which are covered by tungstate–titanate particles. The TEM images proved that Pt-WO<sub>3</sub>-TiO<sub>2</sub>/C composite

uniformly dispersed on the carbon particle, the Pt particles size appeared in the range of 2 to 3 nm, and prepared 10 % Pt/C catalyst shows the spherical shape of Pt particles. 10 % Pt/C commercial catalyst shows some degree of aggregation of the particles. The XRD analysis result of platinum nanoparticle size was confirmed by the TEM analysis results.

## Conclusions

This study has successfully developed a novel method for preparation of nano-sized carbon-supported Pt-WO<sub>3</sub>-TiO<sub>2</sub> electrocatalysts with various compositions (as weight percentage, Pt-W-Ti 0:5:5, 2:4:4, 4:3:3, 6:2:2, 8:1:1, and 10:0:0) of ternary nanocomposite electrocatalyst as anode material. The electrocatalytic activities of optimized Pt-WO<sub>3</sub>-TiO<sub>2</sub> (type “C”) nanocomposite anodic oxidation have shown better performances than 10 % Pt/C and commercial 10 % Pt/C in PEMFC. X-ray diffraction characterization was carried out to determine the crystalline size. Electrochemical experiments including cyclic voltammetry were also conducted to characterize these Pt-WO<sub>3</sub>-TiO<sub>2</sub> (Pt-W-Ti 4:3:3 catalysts) and to determine the electrochemical surface area of the catalyst. The amount of Pt was reduced, as per the main objective of the present work, from 1.76 to 0.704 mg cm<sup>-2</sup>. Through this work, it is established that the presence of WO<sub>3</sub>-TiO<sub>2</sub> molecules enhances the proton transport within the platinum surface through the inclusion of WO<sub>3</sub>-TiO<sub>2</sub> molecules into Pt particles. The effective utilization of platinum is much higher than 10 % Pt/C, when WO<sub>3</sub>-TiO<sub>2</sub> molecules are introduced with Pt nanoparticles, paving the way for achieving cost-effective PEMFC containing reduced loadings of the noble metal, platinum.

**Acknowledgments** The authors thank the M/s. High Energy Batteries (India) Ltd., Mathur 622 001, Tamil Nadu, India for the encouragement and support.

## References

- Martínez-Huerta MV, Rojas S, Gómez de la Fuente JL, Terreros P, Peña MA, Fierro JLG (2006) Effect of Ni addition over PtRu/C based electrocatalysts for fuel cell applications. *Appl Catal B Environ* 69:75–84
- Park K-W, Choi J-H, Kwon B-K, Lee S-A, Sung H-Y, Ha H-Y, Hong S-A, Kim H, Wieckowski A (2002) Chemical and electronic effects of Ni in Pt/Ni and Pt/Ru/Ni alloy nanoparticles in methanol electrooxidation. *J Phys Chem B* 106:1869–1877
- Grgur BN, Markovic MM, Ross PN (1998) Electrooxidation of H<sub>2</sub>, CO and H<sub>2</sub>:CO mixtures on a well-characterized Pt70Mo30 bulk alloy electrode. *J Phys Chem B* 102:2494–2501
- Ren X, Springer TE, Zawodzinski TA, Gottesfeld S (2000) Methanol transport through nafion membranes, electro-osmotic drag effects on potential step measurements. *J Electrochem Soc* 147 (2):466–474



5. Hayden BE (2003) Single-crystal surfaces as model platinum-based hydrogen fuel cell electrocatalysts. In: Wieckowski A et al (eds) *Catalysis and electrocatalysis at nanoparticle surfaces*. Marcel Dekker, New York, pp 171–210
6. Mukerjee S (2003) In-situ X-ray absorption spectroscopy of carbon-supported Pt and Pt-alloy electrocatalysts: correlation of electrocatalytic activity with particle size and alloying. In: Wieckowski A et al (eds) *Catalysis and electrocatalysis at nanoparticle surfaces*. Marcel Dekker, New York, pp 501–530
7. Li J-H, Fan L-Z, Liao L-B (2010) Electrodeposition of platinum on tourmaline and application as an electrocatalyst for oxidation of methanol. *Ionics* 16:33–38
8. Rajalakshmi N, Lakshmi N, Dhathathreyan KS (2008) Nano titanium oxide catalyst support for proton exchange membrane fuel cells. *Int J Hydrogen Energy* 33:7521–7526
9. Guo JW, Zhao TS, Prabhuram J, Chen R, Wang CW (2005) Preparation and characterization of a Pt-Ru/C nanocatalyst for direct methanol fuel cells. *Electrochim Acta* 51:754–763
10. Antolini E, Salgado JRC, Gonzalez ER (2005) Carbon supported Pt75M25 (M=Co, Ni) alloys as anode and cathode electrocatalysts for direct methanol fuel cells. *J Electroanal Chem* 580:145–154
11. Srinivasan S, Ticianelli EA, Derouin CR and Gottesfeld S (1988) Methods to attain high power density in SPE fuel cells with low-platinum -loading electrodes. 1988 Fuel Cell Seminar, Program and Abstracts, California, pp. 324–327
12. Travitsky N, Ripenbein T, Golodnitsky D, Rosenberg Y, Burshtein L, Peled E (2006) Pt-, Pt-Ni- and PtCo-supported catalysts for oxygen reduction in PEM fuel cells. *J Power Sources* 161:782–789
13. Svehla G (1987) *Vogel's qualitative inorganic analysis*, 6th edn. Longman Group Ltd., London, pp 246–286
14. Hoogers G (2002) Fuel cell components and their impact on performance. In: Hoogers G (ed) *Fuel cell technology handbook*. CRC Press, Boca Raton, pp 4.1–4.27
15. Guo JW, Zhao TS, Prabhuram J, Chen R, Wong CW (2006) Development of PtRu-CeO<sub>2</sub>/C anode electrocatalyst for direct methanol fuel cells. *J Power Sources* 156:345–354
16. Trasatti S, Petrii OA (1992) Real surface area measurements in electrochemistry. *Pure Appl Chem* 63(5):711–734
17. He CZ, Kunz HR, Fenton JM (1997) Evaluation of platinum-based catalysts for methanol electro-oxidation in phosphoric acid electrolyte. *J Electrochem Soc* 144:970–979
18. Wang ZB, Yin GP, Shi PF (2006) New Pt-Ru solid compounds as precursors of anodic catalysts for direct methanol fuel cell. *J Alloys Compd* 420:126–132
19. Giorgi L, Pozio A, Bracchini C, Giorgi R, Turtu S (2001) Investigation of ethanol electrooxidation on a Pt-Ru-Ni/C catalyst for a direct ethanol fuel cell. *J Appl Electrochem* 31:325–334
20. Wang ZB, Yin GP, Zhang J, Sun YC, Shi PF (2006) H<sub>2</sub> and H<sub>2</sub>/CO oxidation mechanism on Pt/C, Ru/C and Pt-Ru/C electrocatalysts. *J Power Sources* 160:37–43